

## Synchrotron Radiation Based Research at the Novosibirsk Scientific Center

K. V. Zolotarev<sup>a, b, c, \*</sup>, A. I. Ancharov<sup>a, d, †</sup>, Z. S. Vinokurov<sup>a, b, c</sup>, B. G. Goldenberg<sup>a, b</sup>, F. A. Darin<sup>a, b</sup>,  
V. V. Kriventsov<sup>a, c</sup>, G. N. Kulipanov<sup>a, b</sup>, K. E. Cooper<sup>a, b</sup>, A. A. Legkodymov<sup>a, b</sup>, G. A. Lyubas<sup>d</sup>,  
A. D. Nikolenko<sup>a, b, c</sup>, K. A. Ten<sup>a, e</sup>, B. P. Tolochko<sup>a, d</sup>, M. R. Sharafutdinov<sup>a, b, d</sup>, A. N. Shmakov<sup>a, b, c</sup>,  
E. B. Levichev<sup>a, b</sup>, P. A. Piminov<sup>a, b</sup>, and A. N. Zhuravlev<sup>a, b</sup>

<sup>a</sup> Budker Institute of Nuclear Physics, Siberian Branch, Russian Academy of Sciences, Novosibirsk, 630090 Russia

<sup>b</sup> SKIF Synchrotron Radiation Facility, Boreskov Institute of Catalysis, Siberian Branch,  
Russian Academy of Sciences, Koltsovo, 630559 Russia

<sup>c</sup> Boreskov Institute of Catalysis, Siberian Branch, Russian Academy of Sciences, Novosibirsk, 630090 Russia

<sup>d</sup> Institute of Solid State Chemistry and Mechanochemistry, Siberian Branch,  
Russian Academy of Sciences, Novosibirsk, 630090 Russia

<sup>e</sup> Lavrentyev Institute of Hydrodynamics, Siberian Branch, Russian Academy of Sciences, Novosibirsk, 630090 Russia

\*e-mail: K.V.Zolotarev@inp.nsk.su

Received November 28, 2022; revised December 15, 2022; accepted January 25, 2023

**Abstract**—The SKIF Synchrotron and Terahertz Radiation Center provides users from various organizations with access to modern analytical techniques using synchrotron radiation beams for a wide range of research work. The general direction in developing the Center is now focused on generating new approaches to using synchrotron radiation.

DOI: 10.3103/S1062873822701635

### INTRODUCTION

The Siberian Center for Synchrotron and Terahertz Radiation on the territory of the Budker Institute of Nuclear Physics (Novosibirsk), is a multiaccess center for shared use and provides opportunities for using synchrotron radiation (SR) and free electron laser radiation in the terahertz spectral range for research groups from other organizations.

Studies with the use of SR have been under way for more than 50 years, so it may be argued that the center is one of the longest operating organizations of this type in the world. The first research with the use of SR at the Center began in the 1970s.

Since the Center is located in Novosibirsk, the convenient geographical location and the high concentration of scientific research institutes of the Siberian Branch of the Russian Academy of Sciences in its immediate vicinity ensure a steady demand for the opportunities to conduct multidisciplinary studies with the use of SR. Scientific groups from Novosibirsk and other major scientific centers of Siberia (e.g., Tomsk, Krasnoyarsk, Irkutsk, Barnaul, and Omsk) are regular users of analytical means organized at the Center.

<sup>†</sup> Deceased.

A qualified user community has been organized at the Center, allowing the efficient use of synchrotron and terahertz radiation in investigations in different scientific fields.

The large number of universities in the cities of the Siberian scientific cluster provides a permanent influx of young users and specialists in organizing research with the use of radiation and engineering support for researchers.

The Center's capabilities in hosting different studies are considered below.

### GENERAL DIRECTIONS OF SKIF ACTIVITIES

As noted above, the main mission of the Center is organizing research with the use of synchrotron and terahertz radiation generated by free electron lasers. Other lines of the Center's operations include

- developing, manufacturing, and operating free electron lasers;
- developing and manufacturing high-field multipole superconducting radiation generators;
- developing and manufacturing magnetic elements for different accelerating systems;

**Table 1.** Main parameters of SR sources at SKIF

	VEPP-3	VEPP-4M, low energy	VEPP-4M, high energy	
Energy, GeV	2	1.9	4.5	
Orbit length, m	72		366	
Type of magnetic structure	FODO		FODO	
Emittance, nm rad	~360	25	145	
Beam current, mA	150	20	20	
Number of clots	1, 2	1, 2	1, 2, 6, 17	
Generation systems	Three-pole shifter (2 T)	Swivel magnet (0.4 T)	Swivel magnet (1 T)	Multipole wiggler (1.95 T, 7 + 2 poles)
Optical features $\beta_x, \beta_y, \eta_x, \text{ m}$	2, 4.5, 0.7	9.64, 7.9, 0.9	7.5, 6.7, 1.15	9.7, 7.9, 1.16
Source sizes $\sigma_x \times \sigma_y, \text{ mm}$	$0.9 \times 0.3$	$2.3 \times 0.1$	$3.5 \times 0.2$	$1.5 \times 0.25$
Critical photon energy, keV	5.3	0.8	12	26.3
Number of output channels	8	1	1	1 (three stations)

- developing and manufacturing unique high-speed X-ray single-coordinate detectors;

- developing the scientific program of the SKIF Siberian Ring Photon Source and participating in the production of systems for the accelerating system and user stations;

- organizing regular international SFR (“Synchrotron and Free Electron Lasers: Radiation, Generation and Applications”) conferences;

- participation in university educational programs of various levels and organizing internships;

- international cooperation.

The shared resource center is registered in the national catalog (<https://ckp-rf.ru/ckp/>), allowing participation in the development program for such centers and receiving subsidies for the development and upgrading of equipment. Annual monitoring of the center confirms its successful functioning, which is in turn confirmed by repeated satisfaction of applications for subsidies. Around 50 user organizations sign a 5-year agreement with the Center every year. Applications for research can be submitted by filling out a special form on the Center website (<https://ssrc.biouml.org/#!>). Approximately 200 applications are registered annually.

### SOURCES OF RADIATION AT SKIF

The Center currently uses two SR sources of radiation: VEPP-3 and VEPP-4M electron accelerators, which form a single accelerator complex. The VEPP-4M accelerator is an electron–positron collider for performing experiments in the field of high-energy physics and allows us to obtain colliding electron and positron beams with energies up to 4.75 GeV. The VEPP-3 stor-

age ring is used to preliminarily accelerate beams to an energy of 2 GeV and sometimes polarize electrons prior to their injection into the VEPP-4M accelerator. Primary electron and positron beams enter the VEPP-3 accelerator with an energy of 360 MeV from a unified Budker injection system that also supplies beams to a VEPP-2000 electron–positron collider.

The VEPP-3 storage ring is equipped with a three-pole shifter for the generation of synchrotron radiation. The radiation is transported to experimental stations through special vacuum channels equipped with special beam collimation systems and radiation gates (radiation output frontends). User stations are located in a special experimental hall measuring around  $7 \times 14 \text{ m}^2$ . There are currently eight output channels in use.

Radiation for research is generated by the VEPP-4M accelerator using a specialized nine-pole wiggler installed in the northern semicircle, along with two swivel magnets. Only the electron direction is used to generate SR. The experimental hall for research with the use of SR on the VEPP-4M accelerator has a much larger area ( $50 \times 15 \text{ m}^2$ ), allowing us to install larger stations.

The main parameters of source storage, generation facilities, and the characteristics of radiation points are presented in Table 1. The spectral characteristics of radiation (in the form of photon flux density) are shown in Fig. 1.

Since the VEPP-3/VEPP-4M storage system is actively used for high-energy physics experiments, and most of the modes in these experiments are not compatible with research with SR, time intervals (runs) are allocated for the latter. The total amount of operating time allocated for work with the use of SR is usually

25% of the total time of the system's operation. The operating modes during runs offer the possibility of simultaneous operations with the use of both storage rings.

The choice of beam energy in both storage rings and the distribution of the operating times and moments of beam change in the storage rings are determined on the basis of the planned research programs and in accordance with user requests that are made before starting a run. The protocol for one run in 2022 is presented in Fig. 2. The graphs show the values of the beam currents on VEPP-3 and VEPP-4M accelerators (the first from graph the top and the third graph, respectively). The energy of the beams is depicted by the color of the shaded areas under the curves of the current strengths. The second graph from the top and the bottom graph show the states of the radiation gates in the radiation output channels and the times of measurements with SR.

### SPECIALIZED STATIONS FOR THE IMPLEMENTATION OF ANALYTICAL TECHNIQUES

This section presents brief descriptions of the experimental stations and the analytical means implemented with the use of these stations.

#### *SR Stations and VEPP-3*

##### *Precision Diffractometry and Anomalous Scattering Station*

The station is mounted at channel no. 2 of the SR output of the VEPP-3 electron storage ring. It is designed for studying the structure and phase composition of polycrystalline materials via X-ray diffraction with high instrument resolution. The station includes a collimation system, a monochromator, a diffractometer, a radiation protection complex, and an experiment automation system. The aperture of the input SR beam is formed by horizontal and vertical input tantalum slits with dimensions of  $\sim 0.1$ – $2.5$  and  $5$  mm, respectively. The distance between the radiation point and the entrance slots of the station is around  $10$  m. A perfectly flat Si crystal with a slot throughout the 111 working plane is used to monochromatize the primary "white" SR beam. The geometric features of the crystal allow us to obtain monochromatic radiation in the  $\sim 0.07$  to  $\sim 0.18$  nm range of wavelengths with monochromatization  $\Delta\lambda/\lambda \sim (1-3) \times 10^{-4}$ . The diffractometer installed at the station is based on two precision Microcontrol goniometers that provide independent sample and detector motion with a minimum angle pitch of  $2\theta = 0.001^\circ$ .

Diffracted radiation is registered by a NaI(Tl) scintillator–FEU-130 photomultiplier scintillation detector. A perfectly flat Ge(111) analyzer crystal oriented at the Bragg angle with respect to the direction of the

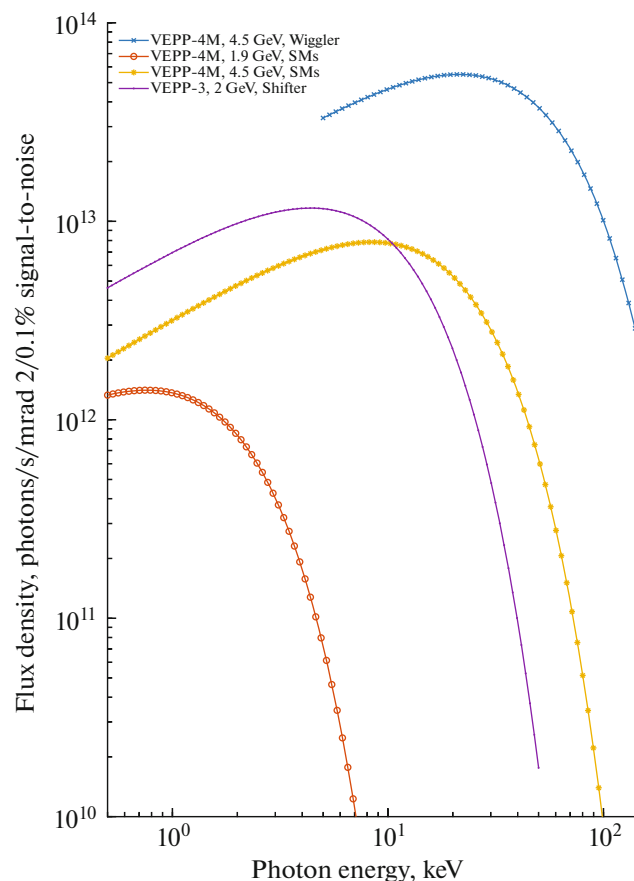


**Fig. 1.** Spectral dependences of the photon flux densities of the main devices for radiation generation in the SCSTR.

diffracted beam is installed in front of the detector. This crystal acts as a narrow receiving slit that provides high instrument resolution of the diffractometer.

The station uses techniques for precisely determining unit cell parameters for polycrystalline materials, X-ray phase analysis, grazing angle diffraction for studying the structure and phase composition of sub-surface layers, determining microstresses and sizes of coherent scattering regions, and hybrid spectral diffraction with the option of arbitrarily choosing the working radiation based on resonance effects near the absorption edges of chemical elements in a structure.

##### *Local and Scanning X-Ray Fluorescent Elemental Analysis Station*

This station is mounted at the third channel of radiation output from the VEPP-3 storage ring. Non-destructive studies on determining elemental composition (from S to U) for natural and man-made samples are performed at this station.

The station consists of several modules: a Si (111) butterfly monochromator, with energy resolution  $dE/E \sim 3 \cdot 10^{-4}$  and operating energy of 6 to 41 keV;

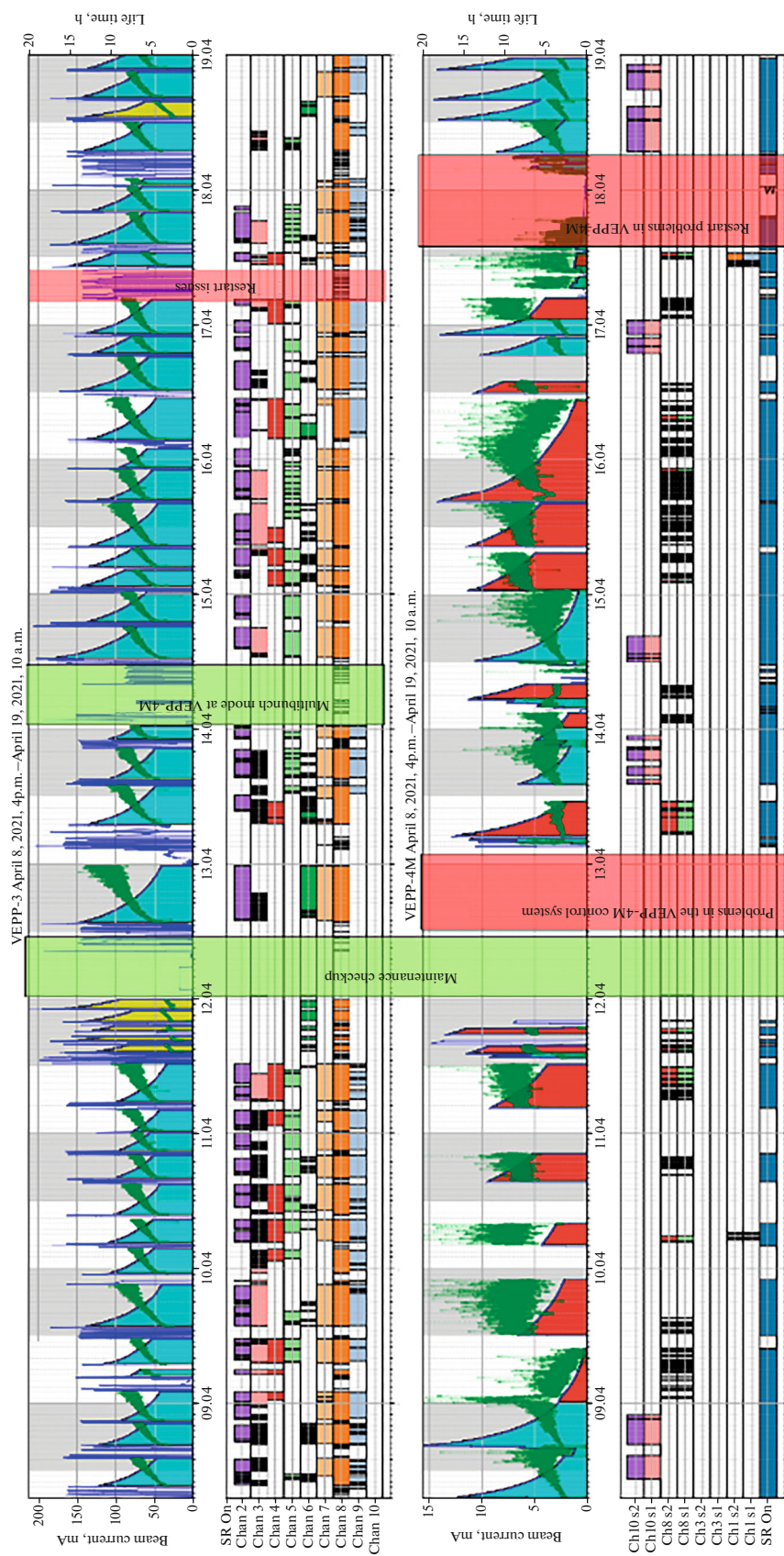


Fig. 2. Protocol for working with SR (run April 8–19, 2022).

systems for collimating and focusing the SR beam in a collimation mode of  $50 \times 50 \mu\text{m}^2$  to  $2 \times 12 \text{ mm}^2$ , along with a focusing mode ranging from  $10 \times 10$  to  $100 \times 100 \mu\text{m}^2$  of a 3D system for moving the sample at a pitch ranging from  $1 \mu\text{m}$  to  $10 \text{ mm}$ ; and Si(Li) Oxford Pentafet, Amptek XR100SDD, and Hitachi Vortex ex-60 detectors. Data are processed with the AXIL and PyMCA software packages. Concentrations are determined with external standards, and there are original procedures for analyses according to fundamental parameters.

Analytical studies can be performed in different experimental modes:

(1) Analysis of discrete and continuous extended samples up to  $300 \text{ mm}$  long. In this mode, extended samples are scanned with a minimum pitch of  $100 \mu\text{m}$ , the beam width on the sample being preset by the exit slits of the monochromator in the range of  $0.05$  to  $11 \text{ mm}$ , and the height is predetermined by a set of slits ranging from  $100 \mu\text{m}$  to  $2 \text{ mm}$ .

(2) Confocal X-ray microscopy (CXM) in 2D and 3D variants. The CRM module allows us to study samples with high spatial resolution in either a single-lens or confocal mode [1]. Studies are performed by moving a sample along three coordinates with a minimum pitch of  $0.1 \mu\text{m}$ , and the maximum size of the relevant area is  $25.4 \text{ mm}$  along the three coordinates. The dimensions of the focal spot on the sample or the confocal volume (for a two-lens mode) can be changed by allowing for the instrumental function of the device [2, 3]. The characteristic dimensions of the confocal volume range from  $10$  to  $50 \mu\text{m}$ .

(3) Total external reflection (TER). Two detectors mounted on the top and side of the sample are used in this mode.

The three measuring techniques described below were developed and certified at the station. They are a way of making measurements when determining the elemental composition of rock samples via X-ray fluorescence analysis using synchrotron radiation taken from the VEPP-3 storage ring [4]; a way of making measurements during an X-ray fluorescence analysis with concentrating optics (polycapillary lenses) [5]; and a procedure for confocal X-ray microscopy in the  $12$  to  $26 \text{ keV}$  range of energies, based on polycapillary optics.

### *High Pressures Station*

This station is installed at the SR channel no. 4 of VEPP-3. It is designed for studying the structure of matter using radiation with an energy of  $33 \text{ keV}$ .

The angles of diffraction are reduced when the wavelength of the X-ray radiation is shortened, and the diffraction maxima shift to the region of small angles. It then becomes possible to register the main set of diffraction maxima using a flat two-coordinate detector. The two-coordinate detector allows us to obtain infor-

mation not only on the position and intensity of diffraction rings, but on the distribution of intensity throughout the ring as well.

For studies performed at the station, we have developed

- in situ diffractometry for studying structural changes that occur during chemical reactions at high temperatures;
- X-ray diffraction studies at high pressures in diamond anvils [6];
- X-ray diffraction studies on the structure of substances at low temperatures;
- X-ray diffraction studies on the structure of matter under conditions of shear and pressure;
- ways of measuring the temperature coefficient of linear expansion for crystalline substances via synchrotron radiation diffraction using a two-coordinate X-ray detector;
- phase analysis of welded seams of micrometer size on aluminum alloys via scanning with an SR beam.

Interesting results have been obtained in recent years:

- Studies of double K-Ca carbonates with different K : Ca stoichiometry in a wide range of P–T revealed interesting features characteristic of mechanisms of structure compression, indicating the limited distribution of alkali metal carbonates in the form of crystalline phases in deep earth conditions.
- The evolution of structural-phase compositions characteristic of welded joints of thermally hardened aluminum and aluminum–lithium alloys was studied using SR, and it was shown that copper-containing stable phases  $\theta(\text{Al}_2\text{Cu})$  and  $\text{S}(\text{Al}_2\text{CuMg})$  form at the dendrite boundary during the laser welding of D16T grade alloy [7].

### *X-Ray Microscopy and Tomography Station*

The X-ray microscopy and tomography station was constructed on the basis of SR output channel no. 5-A of the VEPP-3 electron accelerator. The SR source is a wiggler with a magnetic field of  $2 \text{ T}$ , located  $15 \text{ m}$  from the position of the object under study. At the station, experiments are under way that allow us to study the structure of a sample at a micrometer level via X-ray radiography, topography and tomography. The capabilities of the station allow us to operate with both monochromatic and polychromatic X-rays.

A silicon single crystal with a cut-out channel and a (111) working plane is used to monochromatize the SR beam, located at a distance of  $12 \text{ m}$  from the radiation source. The monochromator allows us to work with the radiation energy spectrum in the range of  $5$  to  $45 \text{ keV}$ . The working area for examining a sample is  $3 \times 3 \text{ mm}^2$ . An ORCA Flash4.0 v3 CCD array with a size of  $2048 \times 2048$  pixels (Hamamatsu) and a GGAG

scintillator 10  $\mu\text{m}$  thick are used to detect X-rays. The reduced pixel size in the optical system of the detector is  $1.65 \times 1.65 \mu\text{m}^2$ . The sampling system allows us to conduct studies at pressures up to 10 MPa and temperatures down to  $-40^\circ\text{C}$  [8].

#### *Diffraction Cinema Station*

The Diffraction Cinema station is installed at SR channel no. 5-B of the VEPP-3 accelerator. It is designed for studying changes in the structure of matter during solid-state chemical reactions under the influence of such external factors as high/low temperatures and pressures, along with weakly scattering objects [9–11].

Monochromatic radiation with  $E/E \sim 10^{-3}$  is cut out from the “white” beam of the synchrotron radiation and focused on the detector using a bent Si(111) crystal. The present wavelength is around 1.5 Å.

The radiation diffracted by the sample is registered using an OD-3 single-coordinate detector or an SX-165 CCD two-coordinate detector. The parallax-free OD-3 detector with a focal length of 350 mm has 3328 channels, a registration angle of  $\sim 30^\circ$ , a maximum load of around 10 MHz, a minimum frame time of 1  $\mu\text{s}$ , along with a maximum number of frames of 64 (at the maximum angular resolution).

The following procedures are implemented at the station:

- powder diffractometry with temporal resolution (cinema mode);
- small-angle X-ray scattering;
- high-temperature diffractometry;
- anomalous scattering at the K-edge of nickel;
- diffractometry of self-propagating high-temperature synthesis [12].

The station has unique equipment:

- an OD-3 single-coordinate detector;
- SX-165 CCD and EIGER2 R 1M two-coordinate detectors;
- a cryogenic helium chamber with a temperature range from 4 to 400 K.

One of the latest experiments at the station was an in situ study on the effect  $\gamma$ -irradiation has on the parameters of macrokinetic synthesis during a thermal explosion [13]. It revealed that the effect of  $\gamma$ -irradiation exerted on a mechanically activated powder mixture with a composition of 64 wt % Ti + Al changes the thermal parameters of combustion because the maximum temperature of synthesis and the rate of combustion are both reduced. The rate of heating the nonirradiated mixture was 204.8 K/s, while that of the irradiated mixture was 81.6 K/s.

The mass fractions of the synthesized compounds are calculated from the preheating stage to the completion of the thermal explosion, depending on time

and temperature. A single-phase equilibrium product with a composition of  $\gamma$ -(TiAl) forms in an  $\gamma$ -irradiated mechanically activated mixture. The synthesized products of combustion obtained without  $\gamma$ -irradiation have such complicated phase compositions as 72%  $\gamma$ -(TiAl), 26% TiAl<sub>3</sub>, and residual Ti (2%).

#### *LIGA Technology and X-Ray Lithography Station*

The station is at the zero (central) channel of radiation output from the shifter on the VEPP-3 storage ring. The station is designed for testing different technological processes:

- deep X-ray lithography in a hard spectrum (from 10 to 20 keV) in thick resistive layers (up to 1 mm or more) for the manufacturing of microstructures, including X-ray masks;
- submicrometer X-ray lithography in a soft spectrum (from 3 to 7 keV at an electron energy of 1.2 GeV) for creating microstructures in thin layers of resists with a topology size of 0.5  $\mu\text{m}$ ;
- studies on the effect synchrotron radiation has on the properties of materials.

The station is equipped with a set of precision micromechanics for precise movement of a sample while recording.

A special mode of operation with a beam energy of 1.2 GeV was developed at the VEPP-3 storage ring in order to perform a number of tasks with soft X-ray radiation.

After adjusting the way of recording a sample, work is done automatically without the participation of operators.

To perform work associated with LIGA technology, the center has a specialized technological room for processing substrates and resists, a so-called clean room (formerly ISO 5, now ISO 6–7) equipped with an air recirculation and purification system, laminar fume hoods (4 pieces), and laboratory equipment for treating and investigating resists:

- a POLI-300 polishing facility;
- a Cookson Electronics SCS P–6708D resist centrifuge;
- a vacuum oven;
- an ultrasound bath for the development of resists;
- an optical profilometer;
- a KEYENCE VHX-5000 optical microscope;
- a Hitachi S-3400N scanning electron microscope.
- a Shimadzu UV-3600 Plus unit.

#### *Submicrosecond Diagnostics Station*

The station is installed at the SR channel no. 0-b of VEPP-3 and is designed for studying such fast processes as detonation, shock waves, and combustion. It

can be used to perform experiments with up to 50 g of an explosive [14, 15].

Polychromatic radiation taken from a wiggler with a field strength of 2 T is used at the station.

A distinctive feature of the station is its use of a VK-005 explosion chamber equipped with thin inlet/outlet beryllium windows for the passage of the SR beam, along with a system for shock wave suppression.

An important element of the station is a Kratky collimator that forms a micrometer-sized background-free beam for experiments using small-angle X-ray scattering or axisymmetric X-ray tomography.

A key feature of the station is a registration system based on a DIMEX fast single-coordinate detector [16]. The registration system ensures the recording of radiation originating from a single bunch of electrons with a duration of 1 ns. Detonation experiments are usually performed with two bunches of electrons in the VEPP-3 unit with a time interval of 125 ns between bunches. In this mode, the detector can register 100 frames with a total time of 12.5  $\mu$ s, which is quite enough for collecting complete information about the detonation process.

Ways of measuring the density distribution (axisymmetric tomography) and small-angle X-ray scattering with a temporal resolution of 1 ns are used at this station.

Studies of two converging shock waves in materials of practical importance to the Zababakhin Scientific Research Institute of Technical Physics have been performed with this station, allowing us to obtain information on their interaction. A similar experiment was performed earlier at the Institute using manganin sensors, but the results could not be interpreted because of their unreliability.

Processes occurring at the outer boundary of metals affected by shock waves (the Rayleigh–Taylor effect, so-called dusting) have also been studied. Nanoparticles in dust flows have been found. Experiments with SR allowed us to assess the Institute's techniques using the laser Doppler effect and piezo sensors. This calibration should allow us to perform experiments at the Institute correctly [17, 18].

This station is equipped with a VK-005 explosion chamber and a PDV laser speed meter.

#### *Precision Diffractometry-2 Station for in situ Polycrystal X-Ray Diffraction*

The station is located at the sixth SR output channel of the VEPP-3 electron storage ring at the SKIF shared resource center. The station's system includes a single-crystal monochromator with the ability to change the radiation wavelength ( $\lambda = 0.10084$ , 0.16467, and 0.17153 nm), a collimation system, and an X-ray diffractometer with an OD-3M single-coordinate position-sensitive detector [19]. The diffractometer is equipped with a XRK-900 high-tempera-

ture reaction chamber (Anton Paar, Austria) and a gas supply system (as many as 3 different gas mixtures at rates up to 200 mL/min) based on SmartTrak 50 gas flow controllers (Sierra Instruments, United States) for investigations in reaction media at temperatures up to 900°C.

It is planned to use a UGA100 quadrupole mass spectrometer (SRS, United States) to control the gaseous environment at the station. It is also possible to use a HTK2000 high-temperature vacuum chamber (Anton Paar, Austria) at the station to perform studies on coatings for heat resistance under vacuum conditions ( $\sim 10^{-4}$  mbar) at temperatures up to 2300°C, along with heat resistance in air (1 atm) at temperatures up to 1500°C. The tasks performed at the station include registering thermally or reaction-induced processes by means of X-ray diffraction with temporal resolutions of 1 s to 5 h [20–22].

#### *Time-Resolved Luminescence Experimental Station*

The Time-Resolved Luminescence station is installed at SR channel no. 6-b of the VEPP-3 facility. The station is designed for the studies with X-ray fluorescence and luminescence with picosecond temporal resolution, along with fast processes in a stroboscopic mode.

The energy of excitation ranges from 3 to 62 keV.

Different techniques have been developed for research performed at the station:

- X-ray fluorescence spectroscopy;
- luminescence with picosecond temporal resolution.

Some interesting results have been obtained in recent years:

- An experimental study on the luminescence of PMMA samples with molecular weights ranging from  $0.2 \times 10^6$  to  $6 \times 10^6$  was performed with SR beam excitation in the 3–60 keV range of energy. It was established that the maximum of the PMMA luminescence band shifts to a longer wavelength (a red shift) as the PMMA molecular weight rises, while the period of luminescence decay is shortened. An increase in the width of the luminescence band with increasing molecular weight was also observed. These effects can be explained by the ordering of the polymer structure and an increase in density, which reduces interatomic distances and thus shifts the energy of electron levels and changes their width [23].

- X-ray fluorescence (XRF) spectra excited in the region of the L-absorption edge of aluminum and the K-absorption edge of beryllium were obtained to establish the role of different cationic sublattices of chrysoberyl  $\text{BeAl}_2\text{O}_4$  in the autolocalization of electronic excitations (EEs). In both cases, signs of the relaxation of cationic excitations were observed in the form of a long-wavelength shoulder of the resonance

peak of exciting photons in the X-ray fluorescence spectra. The energy loss for EE relaxation, determined from the long-wavelength shoulder, was greater for the relaxation of cationic excitons excited in the beryllium sublattice.

We may therefore conclude that both cationic sublattices participate in EE relaxation inside chrysoberyl crystals. Based on a comparison of the energy loss due to the autolocalization of excitons in the photoluminescence spectra (PLS) and X-ray fluorescence spectra (XFS), we may assume the intrinsic luminescence band of 3.9 eV characteristic of  $\text{BeAl}_2\text{O}_4$  crystals is caused by the radiative decay of anionic autolocalized excitons (ALE) in beryllium–oxygen tetrahedra, while the 5.2 eV luminescence band is due to SLE decay in aluminum–oxygen polyhedra [24].

#### *EXAFS Spectroscopy Experimental Station*

This station is based on the eighth channel of the radiation output from the VEPP-3 unit and is designed for obtaining X-ray absorption spectra (XANES and EXAFS) of different samples (normally X-ray amorphous ones) in the liquid phase, solid, and highly dispersed states. The data obtained with the station allow us to determine the electronic structure and structural parameters of the local environment (coordination numbers, interatomic distances) characteristic of the atoms under study, including structural data on samples when X-ray structural means are unacceptable.

The main technical characteristics of the EXAFS-spectroscopy station are a list of chemical elements intended for studies starting from Ti; an operating energy of 4 to 33 keV; an error of 0.2% in measuring the coefficient of X-ray absorption; the concentrations of studied elements ranging from 0.01 to 100 wt %; determination of interatomic distances ranging from 1.5 to 8 Å ( $\pm 1\%$ ); a  $\pm 10\%$  error in determining coordination numbers; and an error of  $\pm 40\%$  in determining the Debye factor.

The facility is now used for XANES and EXAFS spectroscopic studies on highly dispersed objects, functional nanomaterials, and catalysts, for which standard X-ray diffraction techniques are not effective. Such features as sample volume, surface, or sub-surface layers can be analyzed, depending on which technique is being used. Three ways of registering XANES and EXAFS spectra are used: registering transmission spectra, registering total photocurrent, and registering the yield of X-ray fluorescence. New techniques have been developed for preparing samples intended for studying reactive compounds and catalysts under inert conditions.

## VEPP-4M SR STATIONS

There are currently six stations operating on the VEPP-4M storage ring. Three are designed for using radiation from a multipole wiggler. The rest are installed at the radiation output channels from the VEPP-4M swivel magnets. The SR stations of VEPP-4M are described below.

#### *VEPP-4 SR Technological Station*

A specialized Technological Station designed for the practical training of university students in the basics of synchrotron research and testing elements of equipment for synchrotron experiments has been installed on channel no. 1 of the SR output from the VEPP-4M storage ring. Students at Novosibirsk universities of various specialties are directly involved in developing the station and testing new techniques as part of term papers and theses. The students participate in designing and assembling, in developing ways of performing experiments, and creating software packages for automating the equipment at the station. The modular concept of building the station allows us to put it into operation gradually by modernizing it in steps, and to implement different research methods.

The modular concept of the station means it is quite possible to change the configuration of experiments, along with that of station development. Training and demonstration work is done at the station to familiarize personnel with the basics of studies using synchrotron radiation:

- safety precautions when performing research with SR;
- measuring the spatial distribution of SR power;
- studying the operation of and adjusting the monochromator in the range of 6–24 keV,
- creating preset radiation parameters for subsequent studies,
- studies of SR interaction with substances (absorption, X-ray fluorescence analysis).

The planned development of the station is based on installing a Mardtb diffractometer equipped with a Pilatus 1M 2D hybrid pixel detector (Dectris, Switzerland). This should allow us to introduce a set of diffraction techniques (powder diffraction analysis and X-ray diffraction analysis of single crystals, including macromolecular crystallography) at the station efficiently.

#### *State of Extreme Matter Station*

This station is installed at SR channel no. 8-b of the VEPP-4 accelerator. The station is designed for studying the behavior of matter at a pressures up to 300 kbar and temperatures up to 10000°C under conditions of detonation and shock-wave loading [25].



Ways of measuring the density distribution (axisymmetric tomography) and small-angle X-ray scattering with temporal resolution of 70 ps are used at the station [26–28].

The distribution of density in the expansion zones of powerful explosives (up to 200 g TNT) that are of practical importance to the Zababkhin Institute has been measured with a temporal resolution of 70 ps and a statistical accuracy of 3%. The data obtained with the station have been used to correct calculations made with the Institute's supercomputer.

Studies on the formation (nucleation) dynamics of detonation products originating from high explosives (200 g of TNT) that are of practical importance to the Institute have been performed for the first time in the world. The size of the measured nucleus nanoparticles ranges from 1 to 600 Å. Such sizes of explosive charges correspond to actual combat charges. This is important because detonation processes depend on the size of the explosive that is used (the scale effect). No such experiments are now under way abroad, but they are planned at the Argonne National Laboratory (United States). The obtained data allowed us to upgrade the codes of the Zababkhin Institute's supercomputer by adding the calculations of the nucleation of detonation products.

Fast single-coordinate detectors developed at the Institute of Nuclear Physics specifically for studying fast processes are being tested at this station [29].

The station is uniquely equipped with a VK-200 explosive chamber, a pneumatic loading facility, and a NANOGATE high-speed camera.

#### *Hard X-Ray Radioscopy Station*

This station is based on SR output channel no. 8 of the VEPP-4M electron accelerator. The SR source is a 9-pole wiggler with a magnetic field of 1.92 T, located at a distance of 33 m from the position of the object under study. The station is designed for research by means of X-ray diffraction, fluorescence analysis, and computer tomography in the hard energy range of 30 to 120 keV. A two-crystal monochromator based on a (111) silicon single crystal operating in a parallel Bragg geometry configuration is used to isolate the working wavelength from the SR energy spectrum.

A Mar345s detector with high quantum efficiency and a dynamic detection range of 17 bits is used to study phase composition by means of X-ray diffraction.

An original system that provides aerodynamic levitation also allows us to heat a spherical sample to the melting temperature, and exclude the possibility of interaction with the cell material. Heating is done with continuous laser radiation, allowing X-ray diffraction studies on the samples at elevated temperatures above 2000°C [30].

The X-ray fluorescence analysis is performed with the use of a Canberra energy-dispersive germanium

detector with a working area of 100 mm<sup>2</sup> and a crystal thickness of 10.5 mm. The SR energy range used at the station allows us to obtain information on the concentration of heavy elements with an accuracy of 1 ppm. When conducting X-ray fluorescence analysis, sample mapping with a pitch of 100 μm can be performed.

The station also offers the opportunity to obtain tomography data concerning the structure of samples up to 100 mm in diameter with a spatial resolution of at least 100 μm [31]. Formography imaging, a DM-20-08K10-00-R detector (Teledyne Dalsa) is used, which allows us to obtain 16-bit wide-format images.

#### *Plasma Station*

The station is installed at the SR channel no. 8-s of the VEPP-4 reactor and is designed for studying the behavior of wall materials of the ITER fusion reactor with Edge-Localized Mode (ELM) instability, accompanied by a 100 J energy release in a time of around 100 ns.

The plates of the ITER diverter must be made of tungsten, which can be destroyed by pulsed heating. The reasons for the formation of cracks are deformations and mechanical stresses caused by an abrupt increase in the temperature of a thin surface layer.

The Plasma Station is designed for the dynamic measurements of deformations and mechanical stresses in tungsten in pulsed heating during ELM dropping, which is modeled by pulsed laser radiation with a duration of 100 ns at an energies up to 100 J and a wavelength of 1 μm. X-ray patterns are registered by a DIMEX fast single-coordinate detector [32].

The first results were obtained for single-crystal tungsten [33]. The observed evolution of the diffraction peak shape was consistent with theoretical predictions based on calculations of strain caused by pulsed heating. The deconvolution of the distribution of residual stress showed good agreement with the theoretical model of strain distribution in a thin surface layer of the sample upon pulsed heating.

Three clearly distinguishable stages in the evolution of the diffraction peak that correlate with the evolution of the temperature and deformation distributions were revealed. Residual plastic deformation grew with subsequent heating pulses and led to the destruction of the sample, accompanied by bifurcation of the observed diffraction peak.

The first experiments for measuring diffraction on polycrystalline tungsten have also been performed. A special detector for this experiment is being developed.

#### *Cosmos Station*

The station was initially designed for perform a wide range of metrological work for calibrating different types of detectors, optical elements, and entire modules operating with soft X-ray radiation. The

wide-range monochromator designed for these purposes used multilayer mirrors and allowed us to cover the spectral range of 30–3000 eV and provide spectral resolution sufficient for most metrological measurements [34, 35]. The monochromator has been also used to perform research in the VUV region. A total external reflection mirror and a diffraction grating were been mounted on the monochromator mechanism.

MgF<sub>2</sub>, which ensures efficient operation in the VUV range of 11.5–23 Å has been used to suppress multiple orders. The spectral sensitivity of three flight samples of the VUSS-E unit was calibrated for Elektro-L space missions 3, 4, and 5 in the period of 2015–2021 using this monochromator [36]. When Si(111) silicon crystals were used in the monochromator, its spectral resolution grew to  $\Delta E/E = 10^{-4}$  throughout the operating range of 2000–9000 eV [37], allowing us to measure the spectral properties (spectral resolution, peak reflection coefficient) of X-ray crystals.

Measurements have been made for RbAP, mica, and silicon crystals. An original two-crystal monochromator with both crystals mounted on one goniometer was also manufactured for make spectroscopic measurements on the Kosmos station. When manufacturing the crystals, The angle between the crystals' surfaces and the Si(111) crystallographic surface was set to 0.3°, while the crystals on the monochromator mechanism were mounted in an antiparallel arrangement.

The directions of total external reflection and the beam, diaphragmed from the crystallographic plane, thus differed from one another by 0.6°, allowing us to avoid long-wavelength parasitic illumination of the detector without filters. This geometric configuration substantially increased the luminosity of the double-crystal monochromator. A series of XAFS spectra measurements near the K-edges of the chemical elements P, S, Cl, Ti, and Cu, and the L-edges of Mo and Nb, were made with a double-crystal monochromator [38–40].

#### ACKNOWLEDGMENTS

This work was done on equipment at the SKIF shared resource center based on the VEPP-4–VEPP-2000 Unique Scientific Facility at the Budker Institute of Nuclear Physics.

#### FUNDING

Our work on improving LIGA-technology, the X-ray Lithography Station, and equipping the Clean Room was done as part of Agreement no. 075-15-2021-1359 with the RF Ministry of Science and Higher Education.

#### CONFLICT OF INTEREST

The authors declare that they have no conflicts of interest.

#### REFERENCES

1. Dar'in, F.A., Rakshun, Ya.V., Sorokoletov, D.S., et al., *Yad. Fiz. Inzh.*, 2017, vol. 8, no. 1, p. 86.
2. Sorokoletov, D.S., Rakshun, Ya.V., and Dar'in, F.A., *Optoelectron., Instrum. Data Process.*, 2015, vol. 51, p. 293.
3. Sorokoletov, D.S., Rakshun, Ya.V., Dar'in, F.A., and Gogin, A.A., *Optoelectron., Instrum. Data Process.*, 2022, vol. 58, no. 1, p. 55.
4. Dar'in, A.V. and Rakshun, Ya.V., *Nauch. Vestn. Novosib. Gos. Tekh. Univ.*, 2013, no. 2(51), p. 112.
5. Dar'in, A.V. and Rakshun, Ya.V., *Nauch. Vestn. Novosib. Gos. Tekh. Univ.*, 2013, no. 2(51), p. 119.
6. Badretdinova, L.K., Kostitsyn, O.V., Smirnov, E.B., et al., *Bull. Russ. Acad. Sci.: Phys.*, 2015, vol. 79, no. 1, p. 15.
7. Malikov, A., Orishich, A., Vitoshkin, I., et al., *J. Manuf. Process.*, 2021, vol. 64, p. 620.
8. Drobchik, A.N., Nikitin, V.V., Fokin, M.I., et al., *J. Synchrotron Radiat.*, 2022, vol. 29, p. 515.
9. Evdokov, O.V., Titov, V.M., Tolochko, B.P., and Sharafutdinov, M.R., *Nucl. Instrum. Methods Phys. Res., Sect. A*, 2009, vol. 603, nos. 1–2, p. 194.
10. Sharafutdinov, M.R., Korchagin, M.A., Shkodich, N.F., et al., *Nucl. Instrum. Methods Phys. Res., Sect. A*, 2007, vol. 575, nos. 1–2, p. 149.
11. Ancharova, U.V., Mikhaïlenko, M.A., Tolochko, B.P., et al., *IOP Conf. Ser.: Mater. Sci. Eng.*, 2015, vol. 81, no. 1, p. 012122.
12. Aleksandrov, V.V., Korchagin, M.A., Tolochko, B.P., and Sheromov, M.A., *Combust., Explos. Shock Waves*, 1983, vol. 19, no. 4, p. 430.
13. Loginova, M., Sobachkin, A., Sitnikov, A., et al., *J. Synchrotron Radiat.*, 2019, vol. 26, p. 1671.
14. Aulchenko, V.M., Zhulanov, V.V., Kulipanov, G.N., et al., *Phys.—Usp.*, 2018, vol. 61, no. 6, p. 515.
15. Ten, K.A. and Aulchenko, V.M., Lukjanchikov et al., *Nucl. Instrum. Methods Phys. Res., Sect. A*, 2009, vol. 603, nos. 1–2, p. 102.
16. Aulchenko, V.M., Baru, S.E., Evdokov, O.V., et al., *Nucl. Instrum. Methods Phys. Res., Sect. A*, 2010, vol. 623, no. 1, p. 600.
17. Ten, K.A., Prueel, E.R., Kashkarov, A.O., et al., *J. Phys.: Conf. Ser.*, 2019, vol. 1147, no. 1, p. 012020.
18. Ten, K.A., Prueel, E.R., Kashkarov, A.O., et al., *Combust., Explos. Shock Waves*, 2018, vol. 54, no. 5, p. 606.
19. Aulchenko, V.M., Evdokov, O.V., Kutovenko, V.D., et al., *Nucl. Instrum. Methods Phys. Res., Sect. A*, 2009, vol. 603, nos. 1–2, p. 76.
20. Rempel, S.V., Eseevich, D., Vinokurov, Z.S., et al., *Ceram. Int.*, 2022, vol. 48, no. 2, p. 2843.
21. Mishchenko, D., Vinokurov, Z., Gerasimov, E., et al., *Crystals*, 2022, vol. 12, no. 3, p. 344.
22. Kaichev, V.V., Vinokurov, Z.S., and Saraev, A.A., *Catal. Sci. Technol.*, 2021, vol. 11, no. 13, p. 4392.
23. Lyubas, G.A., Tolochko, B.P., Ancharov, A.I., et al., *AIP Conf. Proc.*, 2020, vol. 2299, p. 050007.
24. Ivanov, V.Yu., Zinin, E.I., and Pustovarov, V.A., *J. Surf. Invest.: X-ray, Synchrotron Neutron Tech.*, 2015, vol. 9, no. 5, p. 1016.

25. Tolochko, B.P., Kosov, A.V., Evdokov, O.V., et al., *Phys. Procedia*, 2016, vol. 84, p. 427.
26. Rubtsov, I.A., Ten, K.A., Prueel, E.R., et al., *J. Phys.: Conf. Ser.*, 2019, vol. 1147, no. 1, p. 012038.
27. Smirnov, E.B., Muzyrya, A.K., Kostitsyn, O.V., et al., *Bull. Russ. Acad. Sci.: Phys.*, 2015, vol. 79, no. 1, p. 20.
28. Prueell, E.R., Ten, K.A., and Tolochko, B.P., *Dokl. Phys.*, 2013, vol. 58, no. 1, p. 24.
29. Aulchenko, V.M., Evdokov, O.V., Shekhtman, L.I., et al., *Nucl. Instrum. Methods Phys. Res., Sect. A*, 2009, vol. 603, nos. 1–2, p. 73.
30. Ivanov, I.A., Dub, V.S., Karabutov, A.A., et al., *Sci. Rep.*, 2021, vol. 11, no. 1, p. 23501.
31. Marusin, V.V. and Kuper, K.E., *Precambrian Res.*, 2020, vol. 340, p. 105627.
32. Aulchenko, V., Shekhtman, L., Zhulanov, V., et al., *Nucl. Instrum. Methods Phys. Res., Sect. A*, 2017, vol. 845, p. 169.
33. Arakcheev, A.S., Aulchenko, V.M., Balash, I.I., et al., *J. Synchrotron Radiat.*, 2019, vol. 26, p. 1644.
34. Nikolenko, A.D., Avakyan, S.V., Afanasiev, I.M., et al., *J. Surf. Invest.: X-ray, Synchrotron Neutron Tech.*, 2012, vol. 6, p. 388.
35. Akhsakhalyan, A.A., Weiner, Yu.A., Garakhin, S.A., et al., *J. Surf. Invest.: X-ray, Synchrotron Neutron Tech.*, 2019, vol. 13, p. 1.
36. Nusinov, A.A., Alekseeva, A.V., Zavertkin, P.S., et al., *Geliogeofiz. Issled.*, 2020, no. 26, p. 31.
37. Zavertkin, P.S., Ivlyushkin, D.V., Mashkovtsev, M.R., et al., *Optoelectron., Instrum. Data Process.*, 2019, vol. 55, no. 2, p. 107.
38. Fedorenko, A.D., Semushkina, G.I., and Peregudova, N.N., *J. Struct. Chem.*, 2021, vol. 62, p. 853.
39. Fedorenko, A.D., Fomenko, I.S., Gongola, M.I., et al., *J. Struct. Chem.*, 2021, vol. 62, p. 1531.
40. Korotaev, E.V., Syrokvashin, M.M., Filatova, I.Y., et al., *AIP Conf. Proc.*, 2020, vol. 2299, no. 1, p. 080004.

*Translated by O. Polyakov*